BMC Oral Health

RESEARCH

Open Access

# Antibacterial effect of femtosecond laser against *Enterococcus faecalis* and *Fusobacterium nucleatum* biofilms on dentin: an in vitro study

Pei Liu[1], Runze Liu[1], Yi Luo[1], Wei Fan[1*] and Bing Fan[1*]

## Abstract

**Background** Removing infectious bacteria biofilms from the root canal system is crucial for a successful endodontic treatment. This study investigated the antibacterial effect of femtosecond laser (fs-laser) against *Enterococcus faecalis* (*E. faecalis*) and *Fusobacterium nucleatum* (*F. nucleatum*) biofilms on dentin.

**Methods** The chemical composition of dentin slices from extracted human teeth was analyzed using FTIR and Raman probes. The morphology of fs-laser ablated dentin grooves was evaluated by an optical profiler, and the fs-laser ablation fluence threshold was obtained by a mathematical model. A correlation between dentin chemical composition and ablation threshold was established. The antibacterial effect of different fs-laser irradiation dosages within the safe threshold on *E. faecalis* and *F. nucleatum* biofilms was firstly evaluated using the growth curve method. The biofilm removal efficacy on dentin and antimicrobial effect in dentinal tubules was further evaluated by CLSM and SEM analysis. The effect of fs-laser irradiation on the microhardness of dentin surface was also evaluated. The fs-laser irradiation process was observed using a spectrometer.

**Results** The peak intensity of phosphate group showed a positive correlation to the fs-laser dentin ablation fluence threshold in both FTIR and Raman spectroscopy. The safe fluence threshold of 1.8 J/cm$^2$ was determined by a prediction model on 20 dentin samples. The antimicrobial effect of fs-laser increased along with the irradiation fluence or time. Both *E. faecalis* and *F. nucleatum* biofilms on dentin could be effectively removed by the fs-laser with 1.5 J/cm$^2$ fluence for 20 s without compromising the microhardness of dentin surface. Meanwhile, fs-laser could also eliminate the bacteria in dentinal tubules. The generation of plasma occurred during the fs-laser irradiation process, and the plasma spectra exhibited distinguishable characteristics between the two kinds of biofilms.

**Conclusions** Fs-laser could effectively remove both *E. faecalis* and *F. nucleatum* biofilms on dentin, along with a notable antibacterial effect in dentinal tubules.

**Keywords** Femtosecond laser, Biofilm, *Enterococcus faecalis*, *Fusobacterium nucleatum*, Root canal

*Correspondence:
Wei Fan
weifan@whu.edu.cn
Bing Fan
bingfan@whu.edu.cn

[1]State Key Laboratory of Oral & Maxillofacial Reconstruction and Regeneration, Key Laboratory of Oral Biomedicine Ministry of Education, Hubei Key Laboratory of Stomatology, School & Hospital of Stomatology, Wuhan University, #237 Luoyu Road, Wuhan 430079, Hubei, China

## Background

Apical periodontitis (AP) is one of the most prevalent dental diseases with a prevalence of 52% in adult population [1]. More than half of the patients with AP suffer from pain, alveolar bone destruction, and even tooth extraction, which seriously affects the life quality [2]. Microbial colonization in root canals has been identified as the primary cause of periapical tissue inflammation and destruction. Exploring effective antimicrobial methods to control intra-canal infection would certainly contribute to the treatment and healing of AP.

*Enterococcus faecalis* (*E. faecalis*), a Gram-positive facultative anaerobe and conditionally pathogenic bacterium, is frequently found in persistently infected root canals [3]. Related studies have extensively reported the *E. faecalis* colonization in failed endodontic cases with a detection rate ranging from 24 to 77% through both culture and PCR-based studies [4, 5]. Moreover, *Fusobacterium nucleatum* (*F. nucleatum*), a Gram-negative anaerobic bacterium, has been frequently detected with high prevalence and abundance in root canals, particularly with primary endodontic infections [6, 7]. Literatures suggest that *F. nucleatum* could facilitate surface adhesion and aggregation of bacteria and activate inflammation and cell death during the process of AP [8].

Due to the pathogenic role of bacteria colonization in root canals, the primary objective of root canal treatment is to eradicate the bacteria from infected root canals. However, the disinfection process faces challenges posed by the bacteria biofilms and the intricate anatomical structure of root canal system [9]. Biofilms are bacterial colonies encased within extracellular polymeric substance (EPS), which consists of polysaccharides, proteins, and nucleic acids. The EPS matrix confers bacterial colonies with a kind of resistance against immune system and various antibacterial agents, rendering it recalcitrant to conventional disinfection methods [4]. Moreover, the intricate root canal structures, such as isthmus, lateral canals, and dentinal tubules, also compromise the effect of disinfection management by harboring infectious bacteria [10]. Hence, exploring effective disinfection strategies to remove biofilms and residual bacteria from root canal system remains a priority of endodontic studies.

Femtosecond laser (fs-laser) is an ultra-short pulse laser ($10^{-15}$ seconds). Its concise pulse duration, which is less than the thermal relaxation time, effectively restricts the generation of thermal effects [11]. Additionally, the fs-laser could deliver a high-intensity laser pulse to bacterial cells, thereby facilitating highly localized and rapid bacteria inactivation. Fs-laser has been reported to have the ability to eliminate various pathogens, demonstrating its potential in infection control [12–15]. However, bacteria mostly exist in the form of biofilms, whereas the previous studies focused on experiments involving planktonic bacteria. To date, there is a lack of research evaluating the efficacy of fs-laser in eradicating biofilms, particularly in dental background. Therefore, the objective of this study is to explore the potential of fs-laser for root canal disinfection through evaluating the dentin ablation threshold of fs-laser as well as the antibacterial efficacy of fs-laser against both *E. faecalis* and *F. nucleatum* biofilms on dentin. The null hypothesis of the study was that the application of fs-laser will not affect the biofilms across both biofilm models.

## Materials & methods

This study was approved by Ethics Committee of School of Stomatology, Wuhan University (WDKQ2024B20) and complied with the Helsinki Declaration. The sample size for each experimental test was based on previous studies, which evaluated the ablation threshold of teeth [16], as well as antibiofilm effect of medicaments [17, 18]. And at least three trials were performed independently to ensure repeatability.

### Dentin slices preparation

Seventy-six dentin slices (30 for ablation threshold determination, 36 for anti-biofilm test, and 10 for microhardness test) were prepared from extracted teeth as previously described [19]. Briefly, dentin slices ($4 \times 4 \times 1$ mm) were sectioned parallel to the occlusal surface from the crown and subjected to ultrasonic bath with 5.25% NaOCl, 17% EDTA, and dd $H_2O$ for 4 min each. All the dentin slices were then used for the following experiments.

### Determination of dentin ablation fluence threshold

#### *General experimental method*

Firstly, 5 randomly selected dentin slices (E group for experiment) were used for establishing the threshold prediction mathematical model. The FTIR and Raman probes were firstly used to detect the chemical composition of each dentin slice. After fs-laser irradiation on the dentin slices, the dentin ablation threshold was calculated using the ablation width square ( $A_w^2$) method. A mathematical model for predicting the dentin ablation threshold based on the chemical composition of dentin was then established. Another 5 dentin slices (V group for validation) were used to validate the mathematical model. The chemical composition and ablation threshold of these dentin slices were obtained as described above. The reliability of the predicted ablation threshold was then evaluated by Bland-Altman analysis. The established mathematical model was ultimately used to assess the ablation threshold of another 20 dentin slices for the determination of safe dentin ablation fluence threshold. Detailed methods for the above experiments are further described in the following sections.

### *Laser irradiation and measurement*

Dentin samples were irradiated by 1030 nm, 600 fs, fiber fs-laser (TCR-1030, Hongtuo, China) with the spatial distribution of Gaussian beam. Experimental setup of the fs-laser ablation system was shown in Fig. 1A. Grooves were made on dentin slices using single scanning line method at a 1 kHz repetition frequency and 142 mm/s scanning speed. The final output power of fs-laser was measured by a power meter (PM100D, Thorlabs, USA) on the sample stage. The fs-laser with an average power of 20 to 100 mW was used for dentin ablation. The light microscope (VHX-7000 N, Keyence, Japan) and scanning electron microscope (SEM; VEGA3 LMU, TESCAN, Czech) were used to observe the surface morphology of dentin grooves. The surface morphology of dentin grooves was further evaluated by an optical profiler (μscan select, NanoFocus AG, Germany) at 5 different regions of the groove.

The ablation width square ( $A_w^2$) method was used to calculate the Gaussian beam waist radius ($\omega_0$) on the dentin surface and dentin ablation threshold by the equation below:

$$A_w^2 = 2\omega_0^2 \ln\left(\frac{F_p}{F_{th}}\right)$$

$F_{th}$ is laser fluence threshold (J/cm$^2$) and $F_p$ is laser fluence peak (J/cm$^2$). According to the equation, the slope of fitted lines gave the value of $2\omega_0^2$ and the intercept is $2\omega_0^2 \ln(F_{th})$.

### *FTIR and Raman spectroscopy*

FTIR spectra were acquired by a spectrometer (Nicolet 5700, Thermo Fisher Scientific, USA) with a 4 cm$^{-1}$ resolution at room temperature (25 ℃). Curve-fitting was performed by Origin 2023 (OriginLab Corporation, USA) to get the chemical composition (Fig. 1B). The number and position of bands were defined based on second-derivative spectra. The absorption peak intensity of the phosphate group ( $PO_4^{3-}$) at 1010 cm$^{-1}$ was considered as the chemical composition of different dentin samples [16].

Raman spectra were acquired by a spectrometer (i-Raman Portable Raman Spectrometer, B&W Tek, USA) with a focused laser spot (95 μm) at 7000 ms integration time and 25 ℃. Acquired spectra were analyzed by BWSpec4 spectroscopic software (B&W Tek, USA). Raman absolute intensity (RAI), Raman relative intensity (RRI), and laser-induced fluorescence intensity (FI) were defined and calculated according to previous study [20]. RAI was the intensity of the $PO_4^{3-}$ at 960 cm$^{-1}$, and RRI was the intensity of the same peak after subtracting the baseline (Fig. 1C).

## Anti-biofilm effect of fs-laser on dentin slices

### *Bacterial cultivation*

*E. faecalis* (ATCC 29212) was grown in brain heart infusion (BHI) broth or on BHI agar plates aerobically at 37 °C. *F. nucleatum* (ATCC 25586) was cultivated in tryptic soy broth supplemented with hemin (5 mg/L) and vitamin K1 (1 mg/L) or on Columbia blood agar plates anaerobically at 37 °C. The optical density($OD_{600}$) of 1 was equivalent to $1 \times 10^9$ colony-forming units (CFUs)/mL.

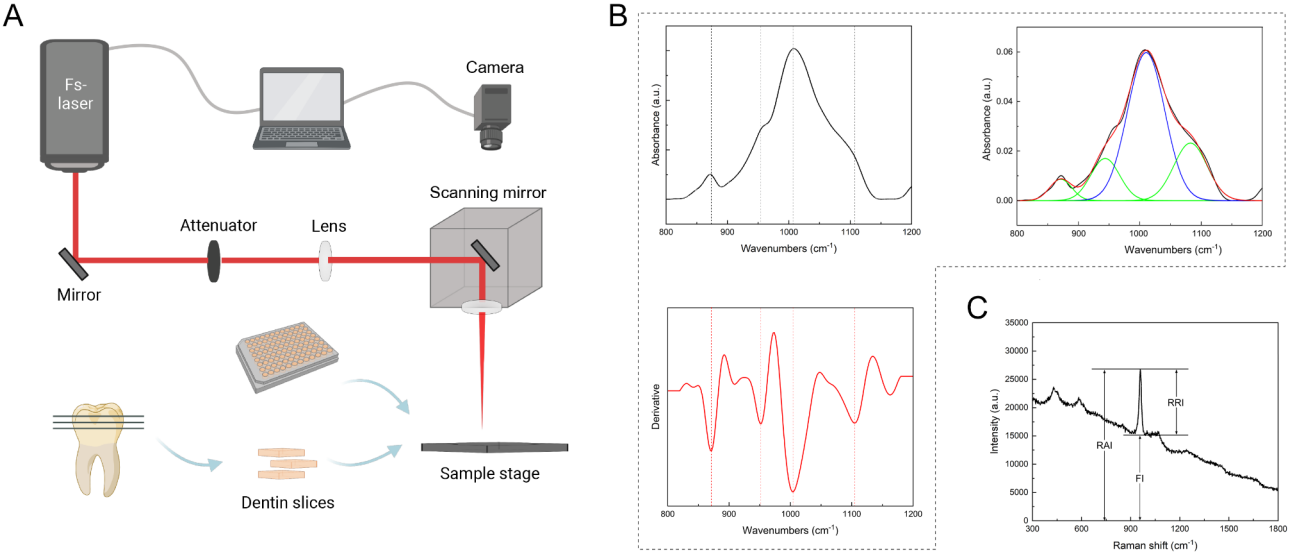


**Fig. 1** Experimental design and chemical composition analysis method. (**A**) Experimental setup of the fs-laser ablation system. (**B**) FTIR analysis procedure. (**C**) Raman analysis diagram

#### *Determination of laser dosage for biofilm removal*

A 200 μL *E. faecalis* or *F. nucleatum* suspension ($1 \times 10^8$ CFUs/mL) was added to a 96-well plate with a glass bottom, and the culture medium was refreshed daily for 7 days. The biofilms were gently rinsed, and the liquid was discarded. Subsequently, biofilm removal was conducted using a fs-laser with a 1 kHz repetition frequency and a 142 mm/s scanning speed. The laser beam was vertically irradiated and scanned line by line following a hatching design with a spot overlap of 29%. The irradiation fluence ranging from 0.5 to 1.8 J/cm$^2$ for 5 to 20 s was used. Then, the wells were supplemented with fresh culture medium and incubated at 37 °C. Treatment of 2.5% NaOCl solution for 20 s served as the positive control, and treatment of normal saline for 20 s was used as the negative control. Each group included 5 repeated wells. The $OD_{600}$ value was detected using a microplate reader (Synergy H1, BioTek, USA). Based on the ablation determined threshold, the 1.5 J/cm$^2$ fs-laser with a duration of 20 s was selected for the following antibacterial experiments on both *E. faecalis* and *F. nucleatum.*

#### *Anti-biofilm effect on dentin slices*

A 3 mL *E. faecalis* or *F. nucleatum* suspension ($1 \times 10^8$ CFUs/mL) and 18 sterilized dentin slices were added in centrifuge tubes for 28 days and the culture medium was refreshed every three days. The 1.5 J/cm$^2$ fs-laser with a duration of 20 s treatment was used for biofilm removal. Treatment of 2.5% NaOCl solution for 20 s served as the positive control. Dentin slices treated with normal saline were used negative control. Each treatment group included six dentin slice samples.

A confocal laser scanning microscope (CLSM, TCS SP8, Leica, Germany) was used on 3 samples of each group to observe the biofilm. The LIVE/DEAD BacLight Bacterial Viability Kit (Invitrogen, USA) and calcofluor white (Sigma-Aldrich, USA) were used as dyes before observation. SEM (MIRA GMS, TESCAN, Czech) was also used on 3 samples of each group to observe the surface of dentin slices.

### Dentin surface microhardness test

Ten dentin slices were randomly allocated into two groups ($n = 5$), with one group subjected to 1.5 J/cm$^2$ fs-laser treatment and the other group treated with 2.5% NaOCl solution. The dentin surface microhardness was firstly detected before the treatments at three randomly selected spots using a microhardness tester (HXD-100TMC/LCD, Taiming, China). Then the microhardness of another three spots close to the pre-treatment three spots was detected after the treatments. The microhardness values before and after the treatments were analyzed and compared between groups.

### Antimicrobial effect in dentinal tubules

The dentin blocks were prepared as previously described [21]. Briefly, nine single-rooted teeth were collected under the ethical approval, and were sectioned into cylindrical root blocks. The cementum of the root blocks was then removed after being longitudinally separated into two halves. Then, the dentin blocks ($4 \times 4 \times 2$ mm) were subjected to a sequential ultrasonic bath of 5.25% NaOCl and 6% citric acid for 4 min each.

Nine sterilized dentin blocks were soaked in 3 mL *E. faecalis* or *F. nucleatum* suspension ($1 \times 10^8$ CFUs/mL) and incubated for 28 days with the medium refreshed every three days. Three dentin blocks were rinsed with normal saline gently and exposed to fs-laser (1.5 J/cm$^2$, 20 s). Another three dentin blocks treated with 2.5% NaOCl solution for 20 s served as the positive control, and the last three dentin blocks treated with normal saline were used negative control. Then, the specimens were vertically split and stained for CLSM bacteria observation.

### Observation of plasma and element spectra induced by fs-laser in biofilms

The plasma and element spectra induced by the irradiation of fs-laser in biofilms were further observed using an experiment platform composed of the laser system, a spectrometer (Avantes, Netherlands), and an intensified charge-coupled device (ICCD, Andor, UK) camera. The experimental parameters were as follows: the laser (wavelength: 1030 nm; fluence: 1.5 J/cm2; repetition rate: 1 Hz), the spectrometer (gate delay: 2 ns; gate width: 9 ns) and ICCD camera (exposure time: 0.1 s; delay: 2 μs; gate width: 9 μs).

### Statistical analysis

GraphPad Prism 8.0 and Origin 2023 was used for statistical analysis and graphing. Data were expressed as the mean ± standard deviation. The Shapiro-Wilk test and Brown-Forsythe test were used to assess the normality distribution and homogeneity of data. For the comparison between the two groups, the independent-samples t-test was used for parametric data. The dentin surface microhardness before and after treatment was compared by paired t-test. For multiple comparisons, the one-way ANOVA was used for parametric data. $P < 0.05$ was considered statistically significant.

## Results

### Observation of ablated dentin grooves

The light microscopy examination revealed no thermal damage phenomenon in ablated dentin grooves, such as melting and carbonization (Fig. 2A). SEM images revealed that the edge of the dentin groove was clean and sharp without molten and smear layers. The side

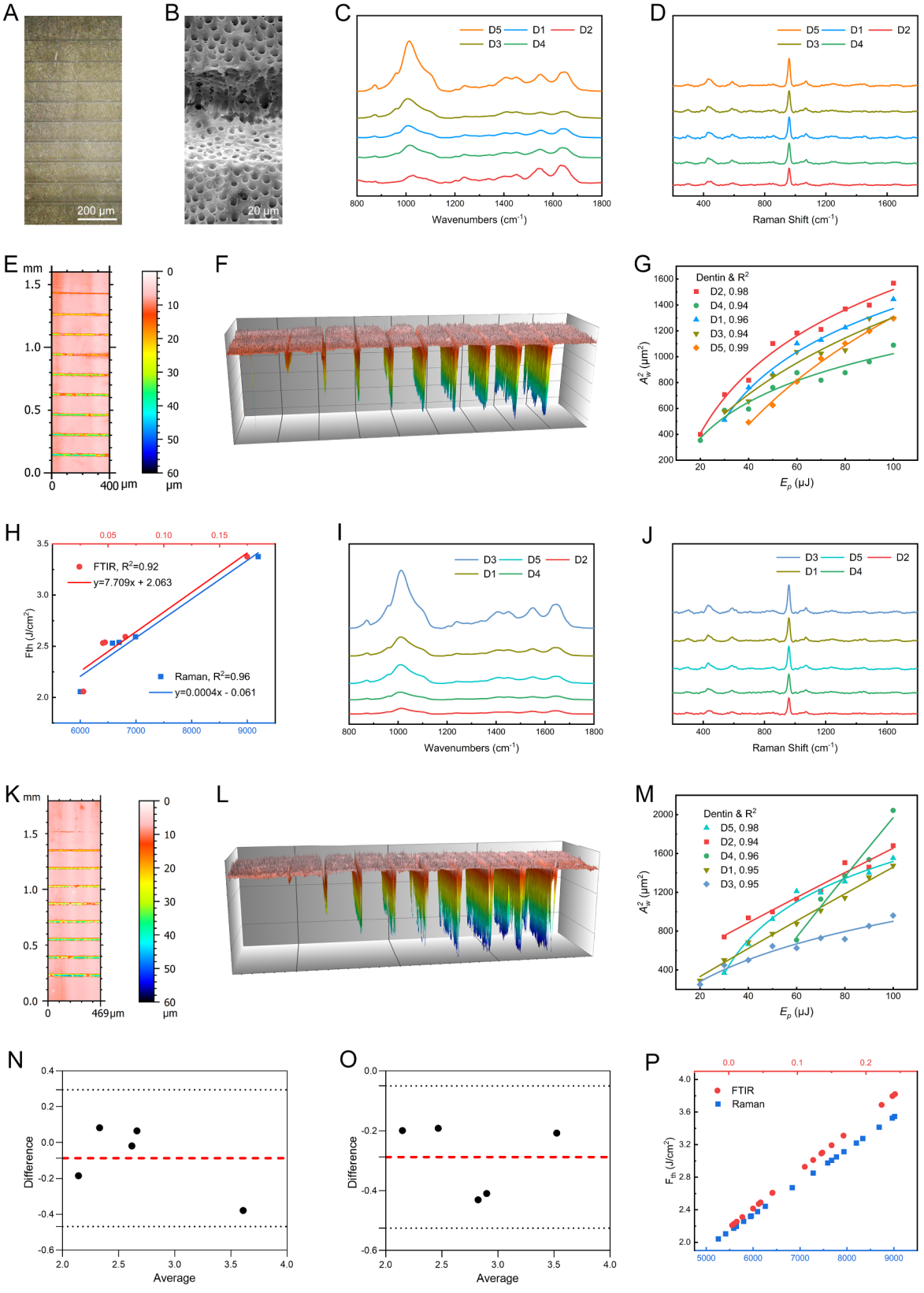


**Fig. 2** (See legend on next page.)

(See figure on previous page.)

**Fig. 2** Determination of dentin ablation threshold. (**A, B**) Morphology of ablated dentin grooves under microscope and SEM. (**C, D**) FTIR and Raman spectra of E group dentin slices. (**E, F**) 2D and 3D profile of ablated dentin grooves on E group dentin slices. (**G**) Linear fitting of $A_w^2$ and pulse energy of E group dentin slices. (**H**) Correlation analysis between chemical composition and ablation threshold. (**I, J**) FTIR and Raman spectra of V group dentin slices. (**K, L**) 2D and 3D profile of ablated dentin grooves on V group dentin slices. (**M**) Linear fitting of $A_w^2$ and pulse energy of V group dentin slices. (**N, O**) Bland-Altman analysis for FTIR and Raman methods. (**P**) Prediction of dentin ablation thresholds

wall structure of the grooves was uniform, and the dentin tubule was completely open (Fig. 2B).

#### Establishment of the correlation between dentin chemical composition and fs-laser ablation fluence threshold

The chemical composition of the dentin slices was obtained using FTIR and Raman probes, and the spectra were shown in Fig. 2C&D. The spectra exhibited a strong peak (1010 $cm^{-1}$ for FTIR and 960 $cm^{-1}$ for Raman), which is associated with $PO_4^{3-}$. The peak intensity of $PO_4^{3-}$ was shown in Table 1.

The optical 2D and 3D profiles of dentin ablated grooves, as shown in Fig. 2E&F, exhibited the width and depth associated with laser power. The $A_w^2$ was plotted against the pulse energy, as shown in Fig. 2G. The trend line equation and ablation parameters of E group dentin slices were shown in Table 1.

To establish the correlation between dentin chemical composition and ablation threshold, the peak intensity of $PO_4^{3-}$ group detected by FTIR and Raman probes were plotted against the ablation threshold (Fig. 2H). The ablation thresholds exhibited a good linear relationship with the peak intensity of $PO_4^{3-}$ group ($R^2 > 0.90$).

#### Determination of dentin ablation fluence threshold

Dentin slices of the V group were used to validate the mathematical model assisted by FTIR and Raman probes. The spectra and peak intensity of $PO_4^{3-}$ group were obtained as mentioned above (Fig. 2I&J). Subsequently, the fs-laser ablation fluence threshold was predicted based on the mathematical model (Table 2).

After the chemical composition analysis, the model validation experiment was conducted. The optical 2D and 3D profiles of dentin ablated grooves were shown in Fig. 2K&L. The $A_w^2$ was plotted against the pulse energy, as shown in Fig. 2M. The trend line equation and ablation parameters of V group dentin slices were listed in Table 3. Bland-Altman analysis was used to evaluate the agreement of the two methods. Figure 2N&O showed that the ablation thresholds predicted based on both FTIR and Raman were well-matched.

Subsequently, the ablation thresholds of 20 dentin samples were analyzed by FTIR and Raman probes. The ablation thresholds were $2.82 \pm 0.61$ J/$cm^2$ for FTIR and $2.75 \pm 0.51$ J/$cm^2$ for Raman; the minimum ablation thresholds were 2.10 J/$cm^2$ for FTIR and 2.05 J/$cm^2$ for Raman (Fig. 2P). The safe threshold of fs-laser was established at 1.8 J/$cm^2$ in this study to avoid damage to dentin.

#### Effect of fs-laser dosage against biofilms

The dosage of fs-laser is influenced by the laser fluence and irradiation time. Therefore, this experiment investigated the effect of different fluence and irradiation time on biofilm removal. As for *E. faecalis* biofilms, fs-laser of 0.5 J/$cm^2$ could not effectively remove it, whereas 1.5 J/$cm^2$ with 15 s duration achieved comparable anti-biofilm efficacy to 2.5% NaOCl. With the increase of fluence, the anti-biofilm effect of 2.5% NaOCl was surpassed by laser irradiation for just 10 s with the fluence of 1.8 J/$cm^2$ (Fig. 3A-D). For *F. nucleatum* biofilms, fs-laser irradiation of 1 J/$cm^2$ for 10 s resulted in a better anti-biofilm effect than 2.5% NaOCl, and 1.8 J/$cm^2$ irradiation for 5 s resulted in almost complete removal of biofilms (Fig. 3E-H).

#### Anti-biofilm effect on dentin

Based on the above results, a 1.5 J/$cm^2$ fs-laser with a duration of 20 s was applied to treat 28-day biofilms on dentin. The CLSM images indicated that fs-laser eliminated *E. faecalis* and EPS on the dentin surface, while dead bacteria were still observed after the treatment with 2.5% NaOCl (Fig. 4A&E). The same results were observed by SEM (Fig. 4B). The dentin surface showed no biofilm structure after the fs-laser irradiation, whereas residual *E. faecalis was* still observed after NaOCl treatment. As for *F. nucleatum* biofilms, fs-laser and NaOCl achieved similar biofilm removal effect (Fig. 4C, D&F).

#### Antimicrobial effect in dentinal tubules

The antimicrobial effect of fs-laser in dentinal tubules was shown in Fig. 5A&D. The fs-laser effectively eliminated both living and dead bacteria from dentinal tubules, leaving only the dentin's background fluorescence. 2.5% NaOCl killed most bacteria in dentinal tubules, with a residual population remaining in the deeper regions. However, 2.5% NaOCl was effective in removing bacteria from the superficial tubule areas. The result is confirmed by CLSM quantitative analysis (Fig. 5B&E). The green fluorescence of live bacteria was significantly reduced after fs-laser irradiation, surpassing that observed with 2.5% NaOCl. Meanwhile, the sterilization depth achieved by fs-laser was twice that of 2.5% NaOCl (Fig. 5C&F, $P < 0.05$).

**Table 1** Peak intensity of $PO_4^{3-}$, trend line equation and ablation parameters of E group dentin slices

| Dentin | Peak intensity of $PO_4^{3-}$ | | Trend line equation | $\omega_0$ (μm) | $F_{th}$ (J/cm$^2$) |
|---|---|---|---|---|---|
| | FTIR | Raman | | | |
| D1 | 0.04720 | 6698.697 | y = 707.09 ln(x)– 1870.9 | 18.80 | 2.54 |
| D2 | 0.02781 | 6001.643 | y = 692.61 ln(x)– 1672.9 | 18.61 | 2.06 |
| D3 | 0.06546 | 6992.187 | y = 621.72 ln(x)– 1578.2 | 17.63 | 2.59 |
| D4 | 0.04539 | 6579.373 | y = 406.14 ln(x)– 848.31 | 14.25 | 2.53 |
| D5 | 0.17478 | 9194.547 | y = 910.12 ln(x)– 2897.1 | 21.33 | 3.38 |

### Effect of fs-laser irradiation on microhardness of dentin surface

Microhardness test revealed that fs-laser treatment did not change the dentin surface microhardness, whereas 2.5% NaOCl solution significantly reduced it (Fig. 6A&B, $P < 0.05$).

### Plasma and element spectra in biofilms

The fs-laser induced plasma in biofilms were observed by ICCD camera. The brightness observed suggested a high plasma density at the central region, indicating it as the primary source of plasma production (Fig. 6C&D). The spectra of plasma generated by fs-laser irradiation on *E. faecalis* and *F. nucleatum* biofilms were displayed in Fig. 5E&F. An average of 29 spectral lines within the range of 200–880 nm for each sample was detected. The elements corresponding to these observed spectral lines were determined against the National Institute of Standards and Technology spectral database. The identified elements included metallic elements (Na, K, Ca, Mg), non-metallic element (C, O, N, P), and molecular bands (C-N) (Table 4). The spectra showed that the two kinds of plasmas exhibited similar elemental composition, albeit with variations in the intensities of certain elements. Specifically, *E. faecalis* biofilms showed stronger intensities for Mg II (279.55 nm), Mg I (285.17 nm), and K I (766.49 nm and 769.90 nm) compared to *F. nucleatum* biofilms (Fig. 6E&F).

**Table 3** Trend line equation and ablation parameters of V group dentin slices

| Dentin | Trend line equation | $\omega_0$ (μm) | $F_{th}$ (J/cm$^2$) |
|---|---|---|---|
| D1 | y = 705.18 ln(x)– 1906.3 | 18.78 | 2.70 |
| D2 | y = 746.26 ln(x)– 1855.1 | 19.32 | 2.05 |
| D3 | y = 390.82 ln(x)– 918.93 | 13.98 | 3.42 |
| D4 | y = 2402.5 ln(x)– 9132.2 | 34.66 | 2.37 |
| D5 | y = 946.48 ln(x)– 2805.8 | 21.75 | 2.61 |

## Discussion

This study provided the evidence that fs-laser irradiation can effectively remove *E. faecalis* and *F. nucleatum* biofilms on dentin and eradicate bacteria within dentinal tubules, without compromising the microhardness or structural integrity of the dentin. The antibiofilm efficacy of fs-laser has been confirmed in both biofilm models, the null hypothesis is rejected. To our knowledge, this is the first attempt to assess the antibiofilm efficacy of fs-laser in an in vitro dentin model, providing insights into fs-laser's potential as a novel disinfection strategy in endodontic treatment.

A key prerequisite for the clinical use of fs-laser in endodontics is establishing its safe dentin ablation threshold, given that damage to dentin is unacceptable. The dentin ablation threshold is intimately linked to the chemical properties of dentin. Carbonated hydroxyapatite, collagen, and water constitute its major components, and their proportions can vary with age, systemic health, and tooth type [22, 23]. In line with earlier reports by Ishii and Loganathan et al., our findings further confirmed that differences in dentin composition could lead to varying fs-laser ablation thresholds [24–26]. Interestingly, this study offered new evidence linking the dentin ablation threshold to the chemical composition of dentin based on the high sensitivity and reproducibility of FTIR and Raman probes [16]. By correlating the intensity of the $PO_4^{3-}$ peak (from FTIR and Raman spectra) with ablation behavior, we established a predictive model that helps refine laser parameters. This approach is especially important given the heterogeneity of dentin, thereby calling for individualized calibration of fs-laser settings in clinical practice.

Previous work indicated that the ablation threshold could vary from 0.44 to 1.6 J/cm$^2$, largely influenced by

**Table 2** Peak intensity of $PO_4^{3-}$ and predicted ablation threshold of V group dentin slices

| Dentin | FTIR | | Raman | |
|---|---|---|---|---|
| | Peak intensity of $PO_4^{3-}$ | Predicted $F_{th}$ | Peak intensity of $PO_4^{3-}$ | Predicted $F_{th}$ |
| D1 | 0.074 | 2.63 | 7914.83 | 3.10 |
| D2 | 0.022 | 2.23 | 5774.25 | 2.25 |
| D3 | 0.225 | 3.80 | 9223.22 | 3.63 |
| D4 | 0.029 | 2.29 | 6560.55 | 2.56 |
| D5 | 0.073 | 2.63 | 7749.27 | 3.04 |

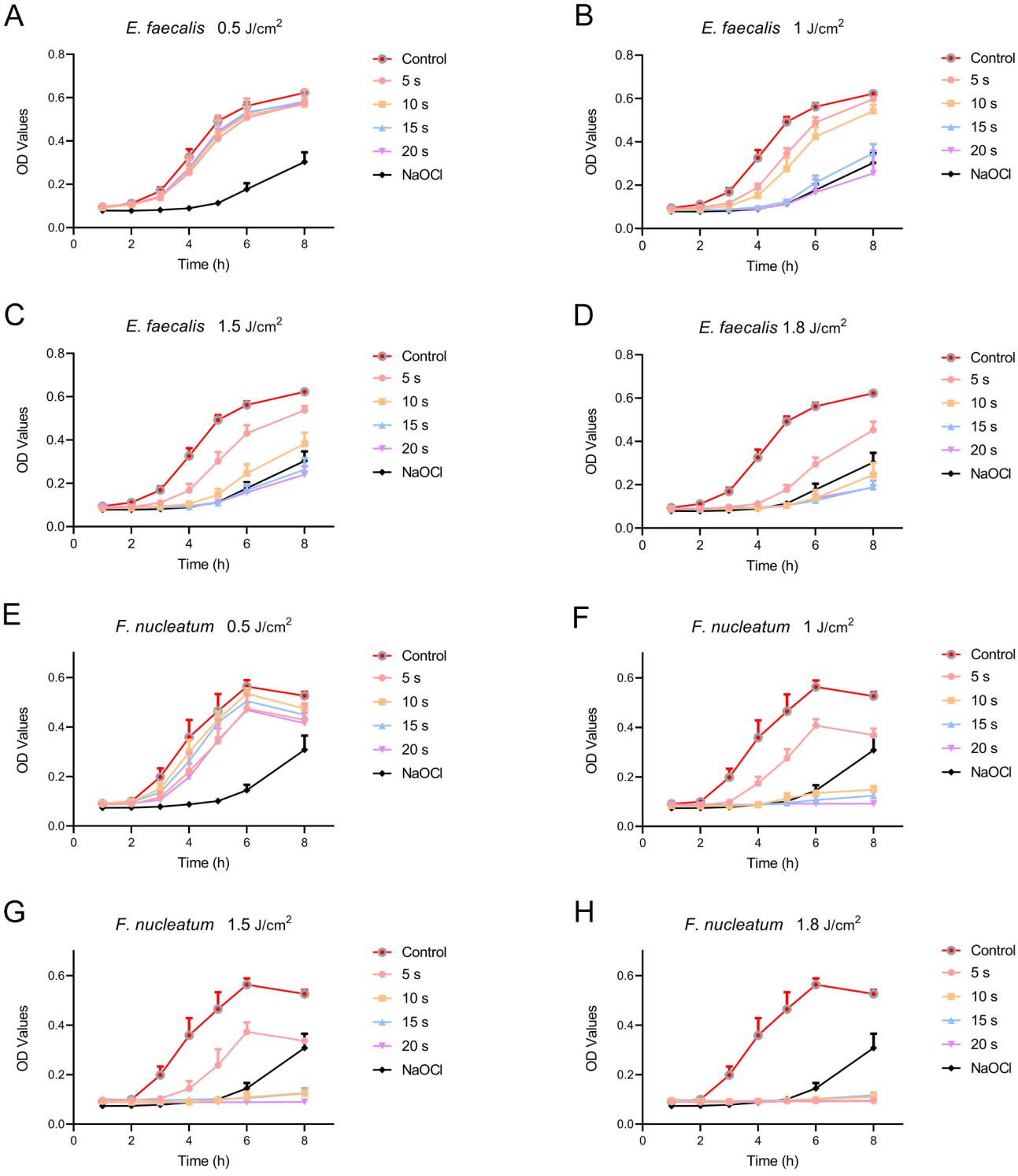


**Fig. 3** Growth curves of fs-laser-treated biofilms. (**A-D**) *E. faecalis* biofilms. (**E-H**) *F. nucleatum* biofilms

different laser parameters such as wavelength, pulse duration, and repetition rate [26–30]. In this study, we determined a threshold of 2.0–3.9 J/cm$^2$ using our fs-laser setup (wavelength 1030 nm, pulse duration 600 fs) and subsequently assessed the antibacterial efficacy at various laser fluences. Consequently, 1.5 J/cm$^2$ for 20 s proved to be the optimal antibacterial dosage that effectively removed biofilms while remaining below the level at which structural or microhardness alterations in dentin would occur. Spot overlap is a critical parameter in

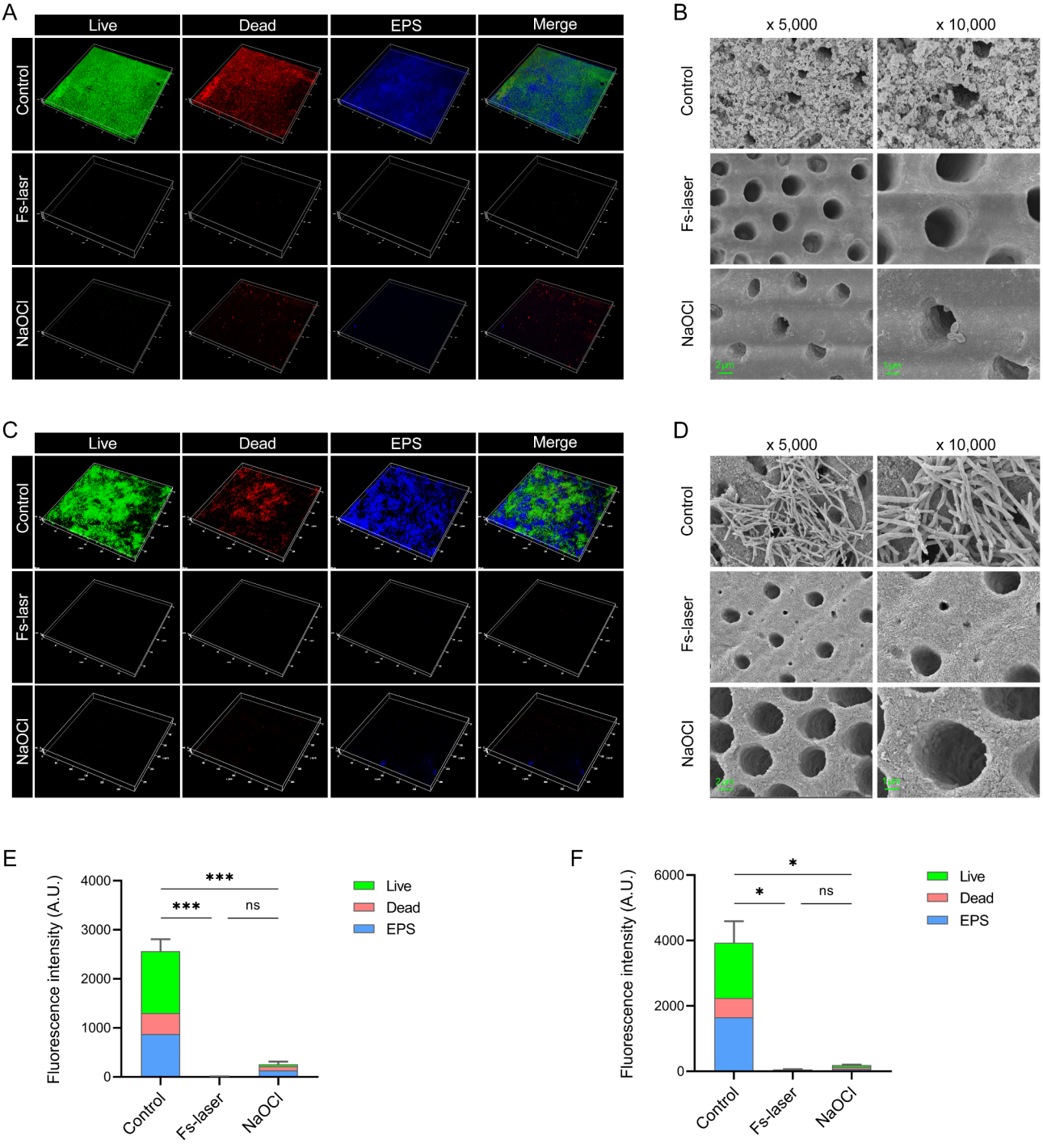


**Fig. 4** Antibacterial effect on dentin surface biofilms. Representative images of CLSM (**A**) and SEM (**B**) for *E. faecalis* biofilms. Representative images of CLSM (**C**) and SEM (**D**) for *F. nucleatum* biofilms. (**E**) Fluorescence intensity of *E. faecalis* biofilms (one-way ANOVA). (**F**) Fluorescence intensity of *F. nucleatum* biofilms (one-way ANOVA). ns, no significance; *, $P < 0.05$; ***, $P < 0.001$

pulsed laser processing, influenced by factors such as repetition rate, scanning speed, and spot diameter. An excessively high spot overlap can lead to heat accumulation, thereby reducing laser processing efficiency and potentially altering the chemical composition of dentin. According to Rapp and Bello-Silva et al., the overlap should be maintained below 50% [31, 32]. Conversely, an overly low spot overlap may result in incomplete coverage, leading to area omission and compromising processing quality. A minimum spot overlap of 29% in this study ensured full coverage while optimizing efficiency and safety for dentin treatment. Our results provided a

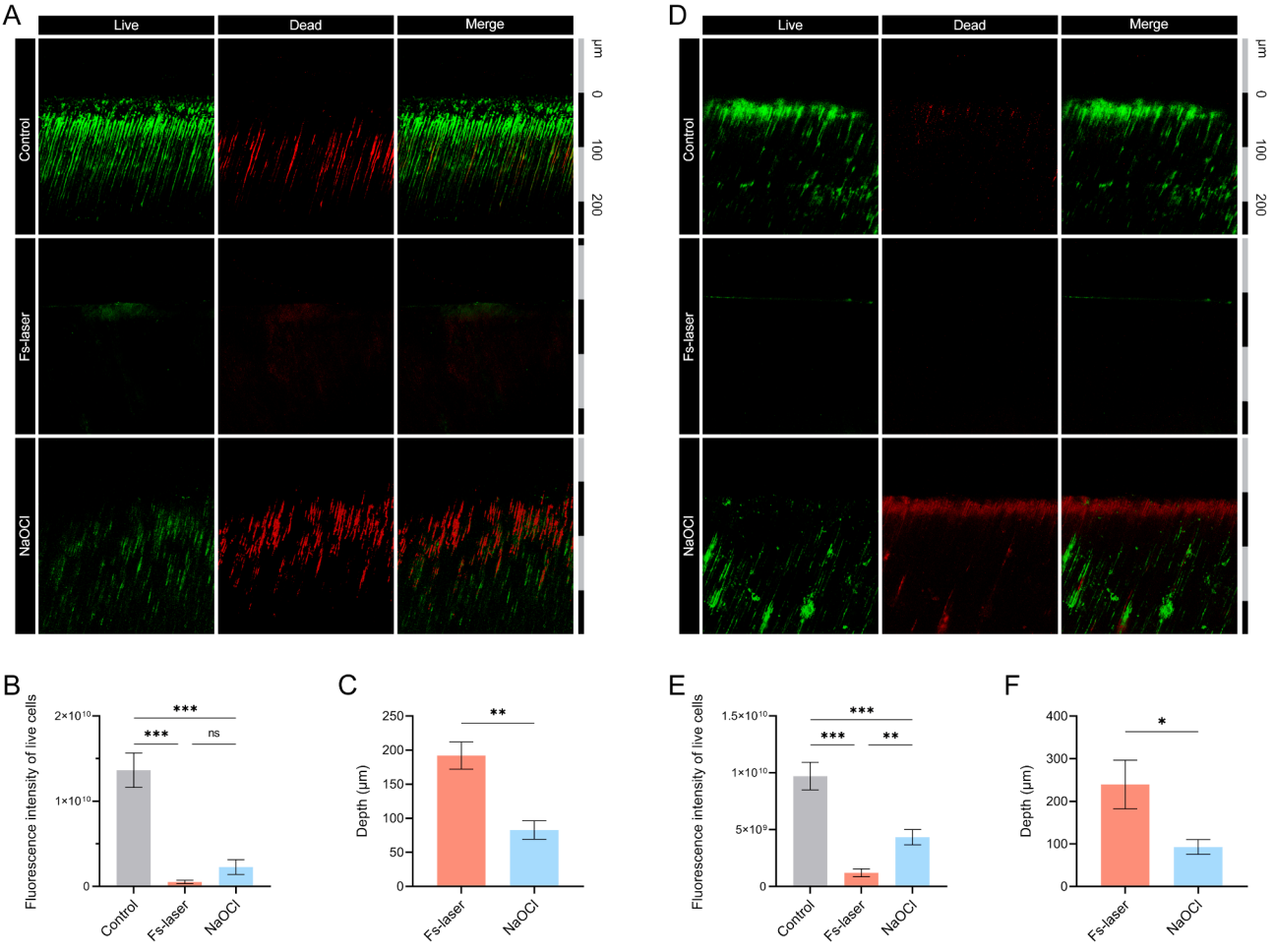


**Fig. 5** Antibacterial effect in dentin tubules. (**A**) CLSM images of dentin tubules infected with *E. faecalis*. (**B**) Quantitative analysis of *E. faecalis* living cells (one-way ANOVA). (**C**) Sterilization depth in dentin tubules infected with *E. faecalis* (independent-samples t-test). (**D**) CLSM images of dentin tubules infected with *F. nucleatum*. (**E**) Quantitative analysis of *F. nucleatum* living cells (one-way ANOVA). (**F**) Sterilization depth in dentin tubules infected with *F. nucleatum* (independent-samples t-test). *, $P < 0.05$; **, $P < 0.01$; ***, $P < 0.001$

foundational parameter set for the clinical application of fs-laser in root canal disinfection.

Unlike many previous studies that tested planktonic bacterial suspensions [12–15], this study systematically assessed the efficacy of fs-laser in eradicating biofilms. Infected root canals normally contain bacteria biofilms, which are more resistant owing to the EPS and complex bacterial aggregation, rather than planktonic bacteria [4, 9, 33]. Studies have revealed a polymicrobial composition in biofilms from infected root canals [6, 7, 34, 35], suggesting that in vitro multispecies biofilm models are more suitable for root canal disinfection studies. However, biofilms sampled from infected root canal cannot always be replicated across different investigations, thereby limiting result comparability and reproducibility [36]. Moreover, the species diversity within these biofilms gradually diminishes with prolonged in vitro cultivation. Amhmed et al. reported that both mono- and multispecies biofilms exhibited similar susceptibility to irrigation [37]. Although *E. faecalis* and *F. nucleatum* biofilms do not fully reflect the microbial diversity of clinical biofilms, they provide a stable and reproducible model on dentin for evaluating biofilm removal, as these two bacteria are key pathogens in primary and secondary endodontic infections [3–7]. Our data indicated that the fs-laser show excellent antibacterial effect against both *E. faecalis* and *F. nucleatum* biofilms, whereas *E. faecalis* exhibited greater resistance to fs-laser than *F. nucleatum*. It is likely due to its thicker cell wall and stronger biofilm formation capacity as well as the absence of free porphyrins that facilitate laser absorption [38, 39].

In this study, we found that the effect of fs-laser on biofilm is primarily a plasma-mediated ablation. The ultrashort pulse duration and extremely high intensity induce a multi-photon absorption process within the material, leading to the ionization of atoms and molecules, which subsequently results in plasma formation [40]. Upon exposure to the fs-laser, the biofilm rapidly transitioned

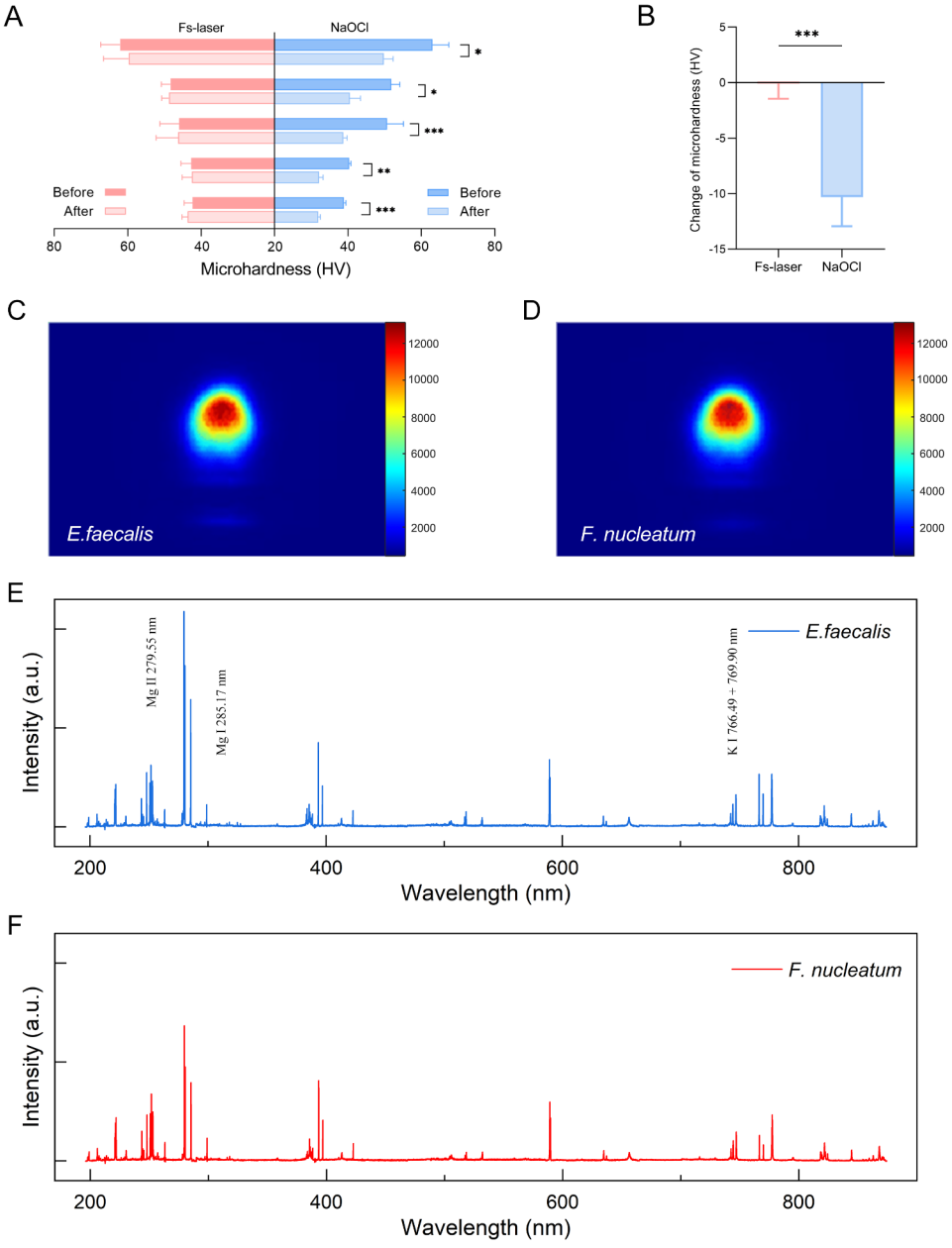


**Fig. 6** Dentin surface microhardness test and plasma observation. (**A**) Comparison of microhardness of dentin surface before and after different treatments (paired t-test). (**B**) Change of microhardness for fs-laser and NaOCl groups (independent-samples t-test). *, $P<0.05$; **, $P<0.01$; ***, $P<0.001$. (**C & D**) Images of laser-induced plasmas. (**E & F**) Plasma element spectra of *E. faecalis* and *F. nucleatum* biofilms

into a plasma state. The distinct differences in the spectra not only indicated that the plasmas originate from two different biofilms but also revealed variations in their compositions. Due to limited thermal diffusion during the plasma's existence, thermal energy remains localized within the plasma region and does not interact with adjacent tissue areas [41]. This highly localized nature allows for a targeted antibacterial effect without structural damage, a notable advantage over higher-temperature laser systems or aggressive chemical agents.

In comparison to NaOCl, often regarded the "gold standard" of root canal irrigants, fs-laser performed similarly or better in removing biofilms, particularly evident in dentinal tubules, where NaOCl penetration can be limited [42, 43]. The 1.5 J/cm$^2$ with a duration of 20 s fs-laser treatment exhibited comparable efficacy of 2.5% NaOCl in eliminating biofilms on the dentin surface. Notably, the efficacy of fs-laser in eliminating bacteria cells in dentinal tubules was superior to that of 2.5% NaOCl, both in terms of depth and cleanliness. In addition, we found that the microhardness of dentin was significantly reduced

**Table 4** Resolved spectral lines of elements and molecular bands

| Elements | Wavelength (nm) | Elements | Wavelength (nm) |
|---|---|---|---|
| C I[a] | 247.86 | Na I | 588.99, 589.59 |
| O I | 777.32, 844.68 | K I | 766.49, 769.90 |
| N I | 742.44, 744.33, 746.94, 818.86, 821.67, 824.34, 868.15 | Ca I | 422.67 |
| | | Ca II | 393.37, 396.85 |
| P II[b] | 531.61 | Mg I | 285.17, 517.23 |
| C-N | 385.47, 386.19, 387.14, 388.34 | Mg II | 279.55, 280.27 |

[a] I represents element atomic line

[b] II represents element ion line

after treatment with NaOCl. Microhardness serves as an indirect indicator of composition alterations in dentin [44, 45], which can affect the bonding properties of the dentin surface, potentially compromising the sealing ability and adhesion of root canal sealers [46]. Insufficient adhesion of root canal filling materials and the absence of a hermetic seal can result in microleakage and bacterial contamination, thereby compromising the success of root canal treatment [47]. In addition, the reduction of dentin microhardness results in less resistant and more brittle substrate, propagating fatigue crack during cyclic stresses [43, 48]. The modification of all these mechanical properties increases the odds of tooth fracture [49, 50]. Unlike NaOCl, microhardness measurements confirmed that fs-laser irradiation did not alter the dentin's mechanical properties. Given the importance of maintaining dentin integrity to prevent post-treatment fractures, fs-laser may present a safer modality for long-term tooth preservation.

Despite these promising findings, several limitations must be acknowledged. Firstly, only monospecies biofilms of *E. faecalis* and *F. nucleatum* were tested, whereas root canals typically harbor multispecies communities. Although multispecies biofilm models are currently difficult to achieve comprehensive microbial diversity analysis, they should be used in future studies. In addition, refinements in laser parameters, including pulse width, wavelength, and scanning strategies, are warranted to optimize both antibacterial effectiveness and preservation of dentin structure. Moreover, further in vivo studies are encouraged to confirm clinical efficacy and safety of fs-laser in root canal disinfection.

## Conclusions

This study provides evidence that fs-laser is capable of efficiently disrupting both *E. faecalis* and *F. nucleatum* biofilms on dentin as well as the bacteria inside dentinal tubules, with minimal risk of dentin damage. These results support the potential clinical application of fs-laser in root canal disinfection, pending further validation in in vivo studies and clinical trials.

### Abbreviations

| | |
|---|---|
| fs-laser | Femtosecond laser |
| AP | Apical periodontitis |
| EPS | Extracellular polymeric substance |
| RAI | Raman absolute intensity |
| RRI | Raman relative intensity |
| FI | Fluorescence intensity |
| OD | Optical density |
| CFUs | Colony-forming units |
| ICCD | Intensified charge-coupled device |

### Acknowledgements

The authors thank the Core Facility of Wuhan University, Research Center for Medicine and Structural Biology of Wuhan University, and Prof. Xiaosun Wang from School of Power and Mechanical Engineering of Wuhan University for their technical support.

### Author contributions

Pei Liu: Conceptualization; Methodology; Investigation; Writing - original draft. Runze Liu and Yi Luo: Investigation; Validation. Wei Fan and Bing Fan: Conceptualization; Writing–review and editing; Supervision; Project administration; Funding acquisition. All authors have read and approved the final manuscript.

### Funding

The research was funded by the National Natural Science Foundation of China (Grant No. 82270968 & 82170943).

### Data availability

All data generated or analyzed during this study are included in this published article.

## Declarations

### Ethics approval and consent to participate

This study was approved by the Ethics Committee of School and Hospital of Stomatology, Wuhan University (WDKQ2024B20) and complied with the Helsinki Declaration. The need for the consent to participate was not applicable and waived by the Ethics Committee of School and Hospital of Stomatology, Wuhan University.

### Consent for publication

Not applicable.

### Competing interests

The authors declare no competing interests.

Received: 6 November 2024 / Accepted: 20 February 2025
Published online: 06 March 2025

### References

1. Tiburcio-Machado CS, Michelon C, Zanatta FB, Gomes MS, Marin JA, Bier CA. The global prevalence of apical periodontitis: a systematic review and meta-analysis. Int Endod J. 2021;54(5):712–35.
2. Falace DA, Reid K, Rayens MK. The influence of deep (odontogenic) pain intensity, quality, and duration on the incidence and characteristics of referred orofacial pain. J Orofac Pain. 1996;10(3):232–9.
3. Godoi-Jr EP, Bronzato JD, Francisco PA, Bicego-Pereira EC, Lopes EM, Passini MRZ, de-Jesus-Soares A, Almeida JFA, Marciano MA, Ferraz CCR, et al. Microbiological profile of root canals indicated for endodontic retreatment due to secondary endodontic infections or for prosthetic reasons. Clin Oral Investig. 2023;27(5):2049–64.
4. Stuart CH, Schwartz SA, Beeson TJ, Owatz CB. Enterococcus faecalis: its role in root Canal treatment failure and current concepts in retreatment. J Endod. 2006;32(2):93–8.

5. Gomes BP, Pinheiro ET, Jacinto RC, Zaia AA, Ferraz CC, Souza-Filho FJ. Microbial analysis of canals of root-filled teeth with periapical lesions using polymerase chain reaction. J Endod. 2008;34(5):537–40.
6. Ordinola-Zapata R, Costalonga M, Nixdorf D, Dietz M, Schuweiler D, Lima BP, Staley C. Taxonomic abundance in primary and secondary root Canal infections. Int Endod J. 2023;56(2):278–88.
7. Ordinola-Zapata R, Costalonga M, Dietz M, Lima BP, Staley C. The root Canal Microbiome diversity and function. A whole-metagenome shotgun analysis. Int Endod J. 2024;57(7):872–84.
8. Lima BP, Shi W, Lux R. Identification and characterization of a novel Fusobacterium nucleatum adhesin involved in physical interaction and biofilm formation with Streptococcus gordonii. Microbiologyopen 2017, 6(3).
9. Siqueira JF Jr., Rocas IN. Present status and future directions: microbiology of endodontic infections. Int Endod J. 2022;55(Suppl 3):512–30.
10. Babeer A, Bukhari S, Alrehaili R, Karabucak B, Koo H. Microrobotics in endodontics: A perspective. Int Endod J. 2024;57(7):861–71.
11. Petrov T, Pecheva E, Walmsley AD, Dimov S. Femtosecond laser ablation of dentin and enamel for fast and more precise dental cavity Preparation. Mater Sci Eng C Mater Biol Appl. 2018;90:433–8.
12. Tsen KT, Tsen SW, Fu Q, Lindsay SM, Li Z, Cope S, Vaiana S, Kiang JG. Studies of inactivation of encephalomyocarditis virus, M13 bacteriophage, and Salmonella typhimurium by using a visible femtosecond laser: insight into the possible inactivation mechanisms. J Biomed Opt. 2011;16(7):078003.
13. Ahmed E, El-Gendy AO, Hamblin MR, Mohamed T. The effect of femtosecond laser irradiation on the growth kinetics of Staphylococcus aureus: an in vitro study. J Photochem Photobiol B. 2021;221:112240.
14. Ahmed E, El-Gendy AO, Moniem Radi NA, Mohamed T. The bactericidal efficacy of femtosecond laser-based therapy on the most common infectious bacterial pathogens in chronic wounds: an in vitro study. Lasers Med Sci. 2021;36(3):641–7.
15. El-Gendy AO, Ezzat S, Samad FA, Dabbous OA, Dahm J, Hamblin MR, Mohamed T. Studying the viability and growth kinetics of vancomycin-resistant Enterococcus faecalis V583 following femtosecond laser irradiation (420–465 nm). Lasers Med Sci. 2024;39(1):144.
16. Loganathan S, Santhanakrishnan S, Bathe R, Arunachalam M. FTIR and Raman as a noninvasive probe for predicting the femtosecond laser ablation profile on heterogeneous human teeth. J Mech Behav Biomed Mater. 2021;115:104256.
17. Siu SY, Pudipeddi A, Vishwanath V, Cheng Lee AH, Tin Cheung AW, Pan Cheung GS, Neelakantan P. Effect of novel and traditional intracanal medicaments on biofilm viability and composition. J Endod. 2024;50(10):1412–9.
18. Shao Y, Zhu W, Liu S, Zhang K, Sun Y, Liu Y, Wen T, Zou Y, Zheng Q. Cordycepin affects Streptococcus mutans biofilm and interferes with its metabolism. BMC Oral Health. 2025;25(1):25.
19. Liu P, Luo Y, Liu R, Fan W, Fan B. Triton X-100 enhanced antibacterial effect of photodynamic therapy against Enterococcus faecalis infection: an in vitro study. Colloids Surf B. 2024;240:113978.
20. Sa Y, Feng X, Lei C, Yu Y, Jiang T, Wang Y. Evaluation of the effectiveness of micro-Raman spectroscopy in monitoring the mineral contents change of human enamel in vitro. Lasers Med Sci. 2017;32(5):985–91.
21. Ma J, Wang Z, Shen Y, Haapasalo M. A new noninvasive model to study the effectiveness of dentin disinfection by using confocal laser scanning microscopy. J Endod. 2011;37(10):1380–5.
22. Kunin AA, Evdokimova AY, Moiseeva NS. Age-related differences of tooth enamel morphochemistry in health and dental caries. EPMA J. 2015;6(1):3.
23. Lizarelli RDZ, Moriyama LT, Jorge JRP, Bagnato VS. Comparative ablation rate from a Er: YAG laser on enamel and dentin of primary and permanent teeth. Laser Phys. 2006;16(5):849–58.
24. Loganathan S, Santhanakrishnan S, Bathe R, Arunachalam M. Surface processing: an elegant way to enhance the femtosecond laser ablation rate and ablation efficiency on human teeth. Lasers Surg Med. 2019;51(9):797–807.
25. Ishii K, Kita T, Yoshikawa K, Yasuo K, Yamamoto K, Awazu K. Selective removal of carious human dentin using a nanosecond pulsed laser operating at a wavelength of 5.85 Mm. J Biomed Opt 2015, 20(5).
26. Loganathan S, Santhanakrishnan S, Bathe R, Arunachalam M. Physiochemical characteristics: A robust tool to overcome teeth heterogeneity on predicting laser ablation profile. J Biomed Mater Res B Appl Biomater. 2021;109(4):486–95.
27. Ji L, Li L, Devlin H, Liu Z, Jiao J, Whitehead D. Ti:sapphire femtosecond laser ablation of dental enamel, dentine, and cementum. Lasers Med Sci. 2012;27(1):197–204.
28. Alves S, Oliveira V, Vilar R. Femtosecond laser ablation of dentin. J Phys D Appl Phys 2012, 45(24).
29. Chen H, Liu J, Li H, Ge W, Sun Y, Wang Y, Lu P. Femtosecond laser ablation of dentin and enamel: relationship between laser fluence and ablation efficiency. J Biomed Opt. 2015;20(2):28004.
30. Loganathan S, Santhanakrishnan S, Bathe R, Arunachalam M. Prediction of femtosecond laser ablation profile on human teeth. Lasers Med Sci. 2019;34(4):693–701.
31. Bello-Silva MS, Wehner M, Eduardo Cde P, Lampert F, Poprawe R, Hermans M, Esteves-Oliveira M. Precise ablation of dental hard tissues with ultra-short pulsed lasers. Preliminary exploratory investigation on adequate laser parameters. Lasers Med Sci. 2013;28(1):171–84.
32. Rapp L, Madden S, Brand J, Maximova K, Walsh LJ, Spallek H, Zuaiter O, Habeb A, Hirst TR, Rode AV. Investigation of laser wavelength effect on the ablation of enamel and dentin using femtosecond laser pulses. Sci Rep. 2023;13(1):20156.
33. Ricucci D, Siqueira JF Jr. Biofilms and apical periodontitis: study of prevalence and association with clinical and histopathologic findings. J Endod. 2010;36(8):1277–88.
34. Arias-Moliz MT, Ordinola-Zapata R, Staley C, Perez-Carrasco V, Garcia-Salcedo JA, Uroz-Torres D, Soriano M. Exploring the root Canal Microbiome in previously treated teeth: A comparative study of diversity and metabolic pathways across two geographical locations. Int Endod J. 2024;57(7):885–94.
35. Arias-Moliz MT, Perez-Carrasco V, Uroz-Torres D, Santana Ramos JD, Garcia-Salcedo JA, Soriano M. Identification of keystone taxa in root canals and periapical lesions of post-treatment endodontic infections: next generation Microbiome research. Int Endod J. 2024;57(7):933–42.
36. Boutsioukis C, Arias-Moliz MT, Chavez de Paz LE. A critical analysis of research methods and experimental models to study irrigants and irrigation systems. Int Endod J. 2022;55(Suppl 2):295–329.
37. Amhmed M, Liu H, Hakkinen L, Haapasalo M, Shen Y. Antimicrobial efficacy of DJK-5 peptide in combination with EDTA against biofilms in dentinal tubules: primary irrigation, recovery and re-irrigation. Int Endod J 2024.
38. Distel JW, Hatton JF, Gillespie MJ. Biofilm formation in medicated root canals. J Endod. 2002;28(10):689–93.
39. Wang S, Wong KI, Li Y, Ishii M, Li X, Wei L, Lu M, Wu MX. Blue light potentiates safety and bactericidal activity of p-Toluquinone. J Photochem Photobiol B. 2022;230:112427.
40. Gamaly EG, Rode AV, Luther-Davies B, Tikhonchuk VT. Ablation of solids by femtosecond lasers: Ablation mechanism and ablation thresholds for metals and dielectrics. Phys Plasmas. 2002;9(3):949–957.
41. Verburg PC, Romer G, in't Veld AJH. Two-temperature model for pulsed-laser-induced subsurface modifications in Si. Appl Phys A-Mater Sci Process. 2014;114(4):1135–43.
42. Dotto L, Sarkis Onofre R, Bacchi A, Rocha Pereira GK. Effect of root Canal irrigants on the mechanical properties of endodontically treated teeth: A scoping review. J Endod. 2020;46(5):596–e604593.
43. Tang W, Wu Y, Smales RJ. Identifying and reducing risks for potential fractures in endodontically treated teeth. J Endod. 2010;36(4):609–17.
44. Arends J, ten Bosch JJ. Demineralization and remineralization evaluation techniques. J Dent Res. 1992;71:924–8.
45. Estedlal T, Omrani LR, Abdi K, Rafeie N, Moradi Z. Development of TiF4-Dendrimer complex gel as an anti-demineralization agent for dentin: an in vitro study. Dent Mater. 2025;41(2):159–68.
46. Neelakantan P, Varughese AA, Sharma S, Subbarao CV, Zehnder M, De-Deus G. Continuous chelation irrigation improves the adhesion of epoxy resin-based root Canal sealer to root dentine. Int Endod J. 2012;45(12):1097–102.
47. Ulusoy OI, Manti AS, Celik B. Nanohardness reduction and root dentine erosion after final irrigation with Ethylenediaminetetraacetic, etidronic and peracetic acids. Int Endod J. 2020;53(11):1549–58.
48. Souza MA, Ricci R, Bischoff KF, Reuter E, Ferreira ER, Dallepiane FG, Quevedo LM, Pereira LHB, Bischoff LF, Hofstetter MG, et al. Effectiveness of ultrasonic activation over glycolic acid on microhardness, cohesive strength, flexural strength, and fracture resistance of the root dentin. Clin Oral Investig. 2023;27(4):1659–64.
49. Uzunoglu E, Aktemur S, Uyanik MO, Durmaz V, Nagas E. Effect of Ethylenediaminetetraacetic acid on root fracture with respect to concentration at different time exposures. J Endod. 2012;38(8):1110–3.

50. Silva e Souza PA, das Dores RS, Tartari T, Pinheiro TP, Tuji FM, Silva e Souza MH Jr. Effects of sodium hypochlorite associated with EDTA and etidronate on apical root transportation. Int Endod J. 2014;47(1):20–5.

## Publisher's note